Surface Review and Letters, Vol. 20, No. 1 (2013) 1350001 (8 pages)

DOI: 10.1142/S0218625X13500017

World Scientific
www.worldscientific.com

PECULIAR SURFACE SIZE-EFFECTS IN NaCl NANO-CRYSTALS

N. KANA*,†, S. KHAMLICH*,†, J. B. KANA KANA‡ and M. MAAZA*,†,§

*Nanosciences African Network, iThemba LABS, National Research Foundation of South Africa, 1 Old Faure Road, Somerset West 7129, Somerset West, Western Cape Province, South Africa

†College of Graduate Studies, University of South Africa (UNISA), Muckleneuk Ridge, Pretoria, South Africa

‡Department of Materials Science and Engineering, University of Arizona, Tucson AZ 85721, USA

§Maaza@tlabs.ac.za

Received 10 July 2012
Revised 18 September 2012
Accepted 1 October 2012
Published 31 January 2013

While the major target of this contribution was the stabilization of the theoretically predicted CsCl form of the sodium chloride which could exhibit a singular and peculiar metallic behavior, this study took advantage of the nano-scaled aspect of the synthesized NaCl to report for the first time in the literature, the size dependence of various thermodynamic parameters of nano-sized NaCl crystals. More accurately, size effect on vaporization temperature of NaCl nano-crystals has been conducted on NaCl nanoparticles exhibiting a net shape anisotropy. The investigated nano-scaled NaCl particles were micrometric in the basal plane while nanometric in the transversal direction. An obvious size variation of the vaporization temperature is observed experimentally in agreement with the theoretical predictions. Specifically, the vaporization temperature T_V decreases from almost 1680 (bulk) to 1290 K (nano-sized): a relative decrease of nearly 23.5%. The $T_V \approx T(\chi)$ size dependence where χ is the relative molar concentration of the initial NaCl precursor was found to follow the form $T_V(^\circ\mathrm{C}) \approx 750.7\chi^2 - 340.1\chi + 1002$.

Keywords: Sodium chloride; size effects; phase transition; surface melting; surface strain; cohesion energy.

1. Introduction

Sodium chloride (NaCl), is the standard rock salt considered in the earliest juncture of X-ray diffraction in the pioneering crystallography and structural investigations.[1] It was the standard system of excellence for cohesion Madelung type energy calculations in the initial stage of solid state physics. Likewise, due to its natural cleavage aptitudes coupled with its perfect surface atomic layering, it has been the preeminent substrate for an extensive period, in the early stages of atomic nucleation and epitaxial growth of thin films in vacuum.[2] Specifically, ⟨100⟩ and ⟨110⟩ faces were extensively used for such a purpose. Within such crystallographic orientations, the crystalline misfit is generally minimal with metals such as Pd(100) and Pt(111) and would be accommodated partly by

strains in the lattices. Similarly, NaCl has a low lattice misfit with numerous semiconductors such as GaAs ⟨110⟩ which is of about 0.4%, assuring good conditions for epitaxial growth. NaCl is also considered as a typical structure for theoretical and computational calculations as it has numerous iso-structural compounds such as, MgO, TiO, KCl and SrS.

Within the current trends in nanosciences and advanced atomic surface probing techniques such as the atomic force microscopy, NaCl with mica crystallographic surfaces are once more a focus pole of fundamental scientific interest. Recently, Sugawara *et al.*[3] confirmed unambiguously the central role of the surface steps and nano-scale faceting of the NaCl and more precisely ⟨110⟩ homo-epitaxial layer in the early stages of the epitaxial crystal growth process. Furthermore, Roberts *et al.*[4] showed that Na ions in the outermost NaCl surface layer are displaced into the surface by 0.12 ± 0.03 Å while the other atomic positions remain within 0.03 Å of the bulk positions. Likewise, investigating nano-structured NaCl structures on standard Ge(100) substrate carried out by low energy electron diffraction and scanning tunneling microscopy by Ernst *et al.*[5] demonstrated that such NaCl systems with thicknesses up to (at least), 15 mono-layers, can be modulated with a period of six lattice constants with an amplitude directed mainly normal to their surface. Above this peculiar structural behavior of NaCl surface in particular in addition to surface effects in general, one should mention the recent challenging theoretical results on bulk NaCl under external pressure perturbations. The structural and electronic properties of NaCl in rocksalt and CsCl phases were investigated under high pressure using total energy minimization techniques. The Kohn–Sham equations were solved within the local density approximation using the pseudo-potential method with a plane wave basis set. The calculated structural properties such as lattice parameter, bulk modulus and its pressure derivative were found to be in reasonable agreement with the experiments. At zero pressure, the rock-salt phase is found to be lower in energy than a hypothetical CsCl structure. However, a phase transition into rocksalt/CsCl atomic arrangement at high pressures was predicted following theoretical electronic band structure at normal and high pressures. It was found that, even, metallization could occur for rock-salt and CsCl structures at such ultra-high pressures.[6] These previous theoretical calculations were not confirmed experimentally due to the difficulty to engineer nano-scaled NaCl crystals. In association with pressure-driven phase transitions, a further specificity of NaCl is the observed unified reduced equation of state which generates a single curve for the P−V behavior at all temperatures as predicted by Thakur and Dwary[7] using various equations of state. These were derived by expanding energy as function of volume in a Taylor series and difference-order Pade approximants combined with quasi-harmonic approximation for free energy. Computerized pressure−volume behavior, isothermal bulk modulus, pressure derivative of bulk modulus and Anderson−Gruneisen parameter of NaCl at high pressure (up to 80 kbar) and various temperatures ranging from 298 to 800 K, were found in a reasonably good agreement with experimental observations in the bulk form and not the nano-scaled one. The ensemble of these previous recent literature attests the new interest generated by NaCl.[3–7]

In its bulk form, NaCl has a cubic unit cell with an f.c.c. lattice type and space group (Fm3m) and a cell parameter (a) of about 5.6410 Å. Its bulk thermodynamic melting and vaporization temperatures are about 1074.5 and 1686 K, respectively. Its bulk modulus and specific heat capacity are of the order of 24.42 GPa and 854 JK^{-1}, respectively. In its nano-sized form, NaCl nano-crystals should exhibit lower surface cohesive energy due to the large ratio of surface ions which leads to a significant reduction of the ionic bonds. This breakdown 3D symmetry at the surface would enhance the surface reactivity of the NaCl as per its ionic bonding type. Therefore, the macroscopic parameters such as the vaporization and/or melting point should decrease with size as predicted theoretically for numerous metallic and semi-conducting materials.[8,9] Similarly, due to the additional surface tension effects, NaCl nano-crystals could exhibit a lower symmetry crystallographic structure. With the intention to investigate possible size effects in NaCl, specifically and related halides in general, one should consent to consider the electric polarizability of the Na^+-Cl^- surface pairs as well as the vibrational surface modes. This assumption is justified again by the 3D symmetry breakdown of the NaCl surface. Indeed, in its nano-scaled form, the surface/volume ratio of NaCl becomes large enough to influence both phonon and electronic properties to a considerable extent. Softer surface phonon modes

should affect the specific heat at low temperatures in particular and thermodynamic melt properties in general. At first glance. if one considers that the surface Na^+-Cl^- pairs acting as independent molecules, their cohesive energy is equivalent to free Na^+-Cl^- molecules i.e. of ≈ -74 kcal/mole. The in-volume Na^+-Cl^- molecules are affected by the Madelung electrical crystal field, their corresponding cohesive energy is bulk related i.e. ≈ -152 kcal/mole. Accordingly, the higher the surface to volume ratio, the smaller is the NaCl crystals and therefore smaller is the melt/vaporization energies. These size effects have been estimated theoretically on the basis of semi-infinite continuum model, semi-infinite lattice dynamic calculations and molecular-lattice dynamics.[10–14] Very early investigations on size effect on the enhancement of specific enhancement in NaCl powder have been performed by Patterson *et al.*[15] The study has revealed indeed an enhancement of the specific heat capacity several times larger than that predicted with the semi-infinite model. While this contribution is targeting the possibility to observe the theoretical phase transition into rocksalt/CsCl atomic arrangement at the nano-scale (excess of surface pressure due to surface tension and coordination effects), it reports, in addition, size-induced effects on vaporization properties of NaCl crystalline nano-platelets.

2. Experiments and Discussion

The NaCl nano-crystals were synthesized by spray-freeze drying processing. To corroborate if there is a direct size effect on melting/vaporization temperatures, a progressive geometrical variation of the NaCl concentration was selected based on the maximum NaCl solubility i.e. 35.7 g/100 ml water at 273 K. High purity sodium chloride (Aldrich, 99.999) was dissolved at room temperature in 300 ml distilled H_2O. Saturated and dilute $NaCl-H_2O$ solutions of different concentrations were prepared and labeled as $NaCl_{1/X}$: $NaCl_{1/1}$ $(0.661 \pm 0.002\,g/ml)$, $NaCl_{1/2}$ $(0.330 \pm 0.002\,g/ml)$, $NaCl_{1/4}$ $(0.165 \pm 0.002\,g/ml)$ and $NaCl_{1/16}$ $(0.041 \pm 0.002\,g/ml)$. Subsequent to an extensive stirring phase, the homogeneous solutions of $NaCl-H_2O$ were sprayed in liquid nitrogen through a sub-micrometric diameter nozzle. For each concentration, the corresponding frozen white ultra-porous network was transferred to a vacuum chamber and placed onto a cooled stage with an initial base pressure of 10^{-3} torr. The corresponding open precursor networks, subsequently, were subjected to a sublimation process by increasing, in a controlled approach, the temperature of the open precursor from 78 K to 373.5 K. The final so-called (lyophilized) precursors were immediately transferred to a dessicator containing silica gel to prevent atmospheric H_2O contamination of the NaCl nano-sized samples. The morphology of the samples was determined by transmission electron microscopy (Siemens 2000). The samples were prepared by placing the nano-sized powders onto standard copper grids coated with carbon film (400 mesh). Powder X-ray diffraction patterns were recorded by employing a Siemens X-ray diffractometer (Cu_{ka}, $\lambda = 1.5418$ Å). Fourier transform infrared spectra were recorded on a Nicolet Impact 410 infrared spectrometer from pure NaCl pellets in the range of $700-4000\,cm^{-1}$. This was followed by thermogravimetric analysis which were carried out using a Mettler Toledo TGA/SDTA851 instrument attached to a mass spectrometer (Balzers Insts) in the range of 293.5–1273 K at a rate of $373.5\,K\,min^{-1}$ under pure argon atmosphere.

The transmission electron microscopy investigations reveal that the different NaCl synthesized nano-particles exhibit a quasi-similar shape morphology even if there is a net difference in the expected agglomeration process. The larger NaCl particles corresponding to the samples denoted $NaCl_{1/1}$ and $NaCl_{1/2}$ samples consist of a set of superposed micrometric cuboidal particles. The smaller NaCl particles related to lower concentration precursor samples i.e. $NaCl_{1/4}$ and $NaCl_{1/16}$, display a cubic shape with perfectly defined edges as illustrated by Fig. 1. More precisely, in this latter case, while the sharp-edged NaCl particles are still micron-sized in the basal plane ($\approx 1-1.7\,\mu m$), they exhibit a net nano-scaled feature in the transversal direction (≈ 62.8 nm). Table 1 summarizes the obtained basal and transversal values. Such a significant shape anisotropy has been confirmed by tilting *in situ* the nano-crystals within the electron microscope sample holder. Such an apparent spatial relief is identical to the surface morphology exhibited by thermally etched NaCl bulk crystal in vacuum.[2] This step-edged spatial construction is expected and is an intrinsic growth property of NaCl specifically and alkali halides clusters in general.[16–18] This step-edge configuration is naturally related to the noteworthy

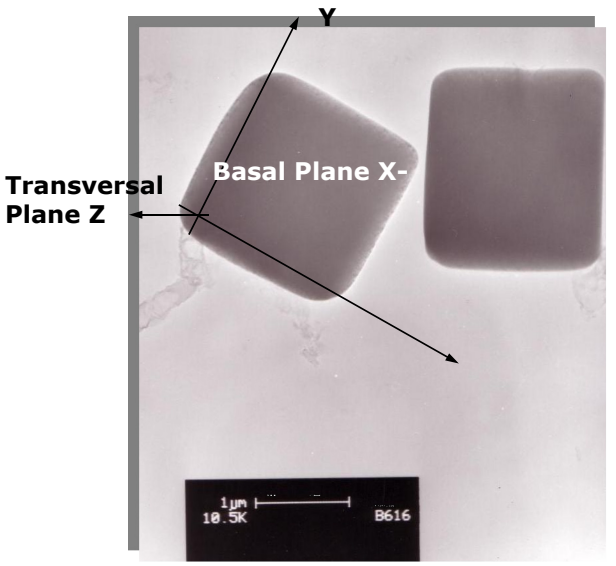

Fig. 1. Transmission electron microscopy of $NaCl_{1/16}$ sample: Basal plane size: $\sim 2 \times 2$ mm, transversal plane: ~ 62.8 nm.

surface electric polarizability of the NaCl nano-crystals. Although there is an obvious evolution in terms of NaCl nano-crystals' shape as well as shape anisotropy with the size, the crystallographic orientation has been found to be identical for all sizes. Figure 2 shows a representative electron diffraction patterns, equivalent to the standard rocksalt bulk $\langle 100 \rangle$ and $\langle 110 \rangle$ orientations. Identical patterns were obtained with all four average sizes. Hence, one should conclude that the surface tension effect, especially on the NaCl nano-platelets i.e. $NaCl_{1/4}$ and $NaCl_{1/16}$ samples, is ineffective to induce a CsCl type or a lower symmetry phase transition at least in our case of this study and within the current transversal dimensions. Taking into account the transversal nano-dimension of the NaCl nano-platelets, one should expect a noteworthy excess of surface

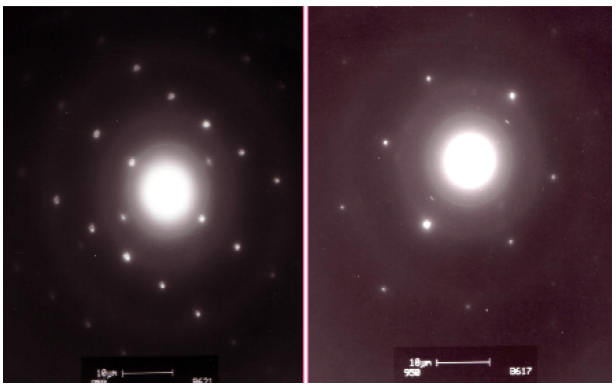

Fig. 2. Typical electron diffraction pattern of NaCl nano-platelets; shown are the patterns of $NaCl_{1/16}$ sample.

pressure, stimulating at least the theoretical predicted structural asymmetry. This is not the case according to the current observed electron diffraction patterns of Fig. 2. The general electron diffraction patterns are identical to the bulk one.

A likely and conceivable explanation could be advanced: the surface tension on the transversal NaCl nano-crystals' faces, could be diminished due to a possible surface adsorbed molecules such as H_2O. To corroborate such a water surface contamination, room temperature infrared spectroscopy measurements were carried out. Figure 3 reports the Fourier transform infrared spectroscopy of the bulk NaCl and nano-sized $NaCl_{1/16}$ sample. Relatively to the bulk NaCl sample, the prominent spectral features of the NaCl nano-sized platelets are typical of surface affected hydroxides. The broad band centered at $\approx 3410\,cm^{-1}$ can be attributed to the hydroxyl groups, which are extensively hydrogen-bonded. The band at ca. $1630\,cm^{-1}$ is assigned to the bonding vibrational modes of a possible surface layer of water molecules. Such an enhanced surface O−H-based contamination is expected due not only to the hygroscopic nature of

Table 1. Average values of the melting $\langle T_{Mel} \rangle$ and vaporization $\langle T_{Vap} \rangle$ temperatures of the synthesized NaCl nano-platelets and their average basal and transversal dimensions.

Sample reference	Relative initial concentration	$\langle T_{Mel} \rangle$ (°C)	$\langle T_{Vap} \rangle$ (°C)	Basal dim. (mm)	Lateral dim. (mm)
1/1	1.0	801	1413	1.3−1.7	108.3
1/2	0.5	333.9	1133	0.9−1.5	91.7
1/4	0.25	117.3	1019.5	0.7−1.2	75.2
1/16	0.0625	29.8	964.8	0.4−0.9	63.5

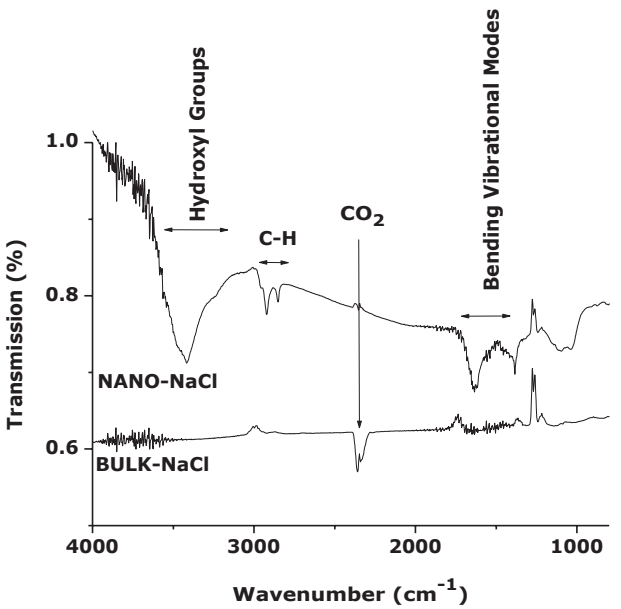

Fig. 3. Room temperature Fourier transform infrared spectra of bulk NaCl and nano-platelets NaCl "$NaCl_{1/16}$ sample."

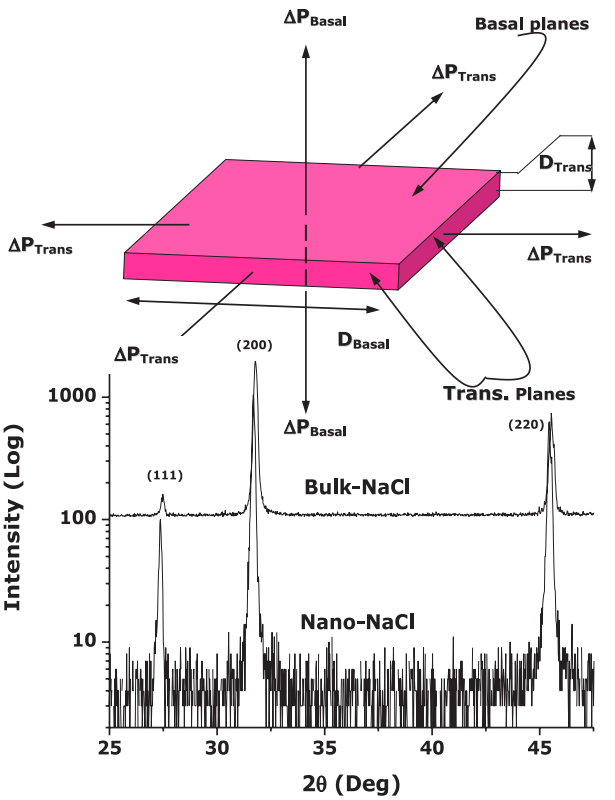

Fig. 4. Room temperature X-ray diffraction patterns of bulk NaCl and nano-platelets NaCl "$NaCl_{1/16}$ sample."

NaCl but also to the high surface/volume ratio as well. Likewise, such a surface adsorption could be favored by the electric polarizability of the Na^+-Cl^- surface ions to be caused by the breakdown of the bulk crystallographic symmetry and its high iconicity degree. In the case of NaCl nano-crystals, these O−H-based surface compounds would contribute naturally and comprehensively to the total cohesive energy. If submitted to an adequate heating, above 373.5 K, these O−H compounds should vaporize. Therefore, above this latter value, the total lattice energy should be diminishing. In a first approximation, this assumption could be supported by the following arguments. As mentioned in the previous introductory part, if the surface Na^+-Cl^- ion pairs could be regarded, behaving as quasi-free molecules, their cohesive energy is equivalent to Na^+-Cl^- monomolecules i.e. of the order of −74 kcal/mol. This rough initial assumption is, in some way, supported by the collapse of the 3D crystallographic symmetry of the substantial population of NaCl nano-particles located at the surface. By contrast, the inner Na^+-Cl^- ions pairs within the NaCl nano-particles, are affected by the Madelung electrical crystal field as in bulk. Their cohesive energy is about −152 kcal/mol. Therefore, as the surface dominates volume in the synthesized NaCl nano-platelets, their melting/vaporization temperatures should be lowered relatively to bulk NaCl as a direct result of many more atoms having lower co-ordination in the nanophase.

The electron diffraction experiments were taken on various crystals but a bi-phase system (Rocksalt and CsCl nano-crystals) could take place. Hence, X-ray diffraction experiments were performed on relatively large amounts for each concentration. Figure 4 reports the room temperature X-ray diffraction pattern of micrometric as well as nanometric NaCl pressed powders corresponding to $NaCl_{1/1}$ and $NaCl_{1/16}$ samples respectively in the angular range of 26°−47° especially. As per noticeably reported, besides the angular shift of the Bragg peaks, the crystallographic and texturing of the NaCl nano-crystals are quasi-similar to bulk. Hence, and in agreement of the previous electron diffraction observations, the CsCl form of the NaCl synthesized crystals, if any, could not be stabilized via size effect at least within the current synthesized nano-platelets. The significant angular shifts of the ⟨110⟩, ⟨200⟩ and ⟨220⟩ Bragg peaks are compatible with an extensive

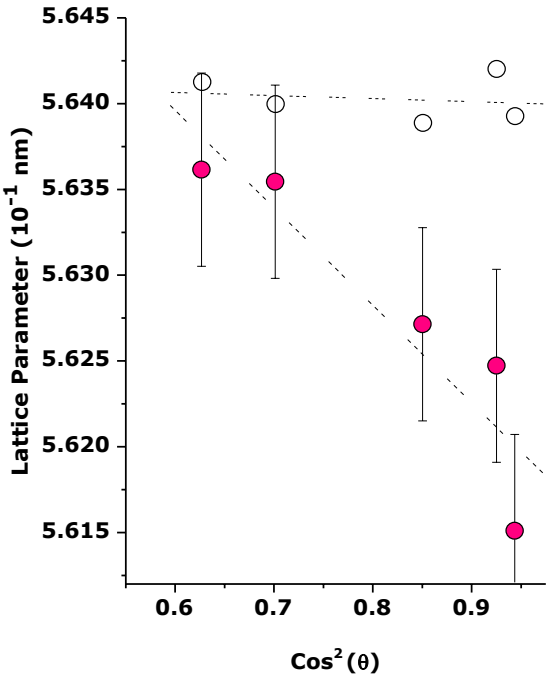

Fig. 5. Angular variation of the crystalline lattice parameter of bulk NaCl "○ ○ ○ ○" and nano-platelets NaCl "● ● ● ●," $NaCl_{1/16}$ sample (line is an eye guide only).

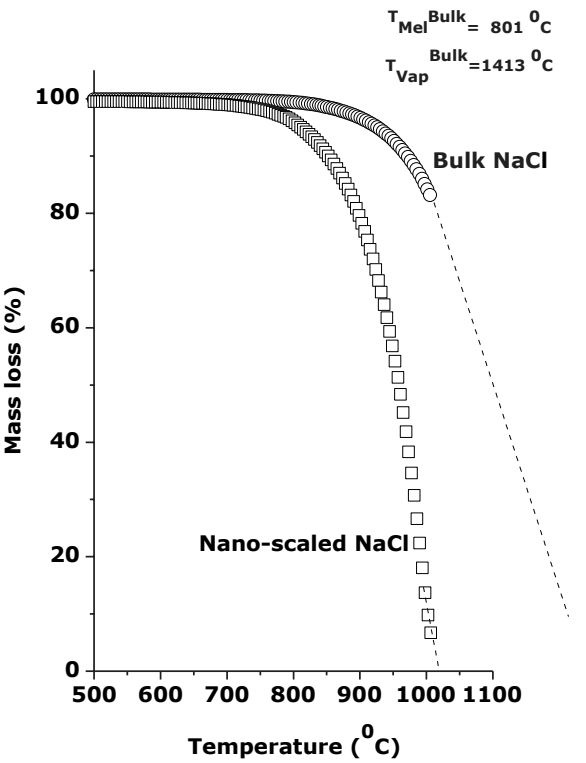

Fig. 6. Thermogravimetry profile of bulk NaCl and nano-platelets NaCl "$NaCl_{1/16}$ sample."

pressure (stress) inducing a noteworthy ⟨110⟩, ⟨200⟩ and ⟨220⟩ reticular planes expansion $\langle Dd_{hkl}/d_{hkl}\rangle$. Figure 5 reports the variation of the deduced lattice parameter $\langle a\rangle \approx \langle d_{hkl}\rangle/\sqrt{(h^2+k^2+l^2)}$ derived for each Bragg peak. The average value ⟨a⟩ is about 5.6280 and 5.6410 Å for bulk and nano-sized NaCl crystals. Therefore, the corresponding relative volume expansion is of the order of $DV/V \approx 0.7\%$. For such a halide material, such a non-negligible value could be correlated to the intrinsic softness of NaCl itself. If one considers that the bulk modulus $B_{NaCl}^{Bulk} \sim 2.4420^{10}$ N/m^2,[21] is alike at the nano-scale, the excess of pressure on the nano-sized NaCl platelets is not far off from $P \approx K\, DV/V \approx 0.17$ GPa. This additional stress pressure is elevated if one considers the results of Miesbauer *et al.*[22] The derived bulk modulus from molecular dynamics calculations was found to be size-dependent with an average value of $B_{NaCl}^{Bulk} = 3.93 \times 10^{10}$ N/m^2 at the nano-scale. Such an elevated bulk modulus value is an agreement with the atomic force microscopy experiments in contact mode.[23] Therefore, the observed excess in the stress pressure in the basal plane on the NaCl nano-platelets is almost 0.30 GPa. Seemingly, such a pressure excess with the nano-scaled size of the engineered NaCl crystals are not sufficient to induce the CsCl form in the current NaCl nano-platelets.

As per the second aim of this contribution in terms of induced size effects on thermodynamic properties in NaCl, the size evolution of both melting and vaporizations temperatures were studied. Figure 6 reports a representative thermogravimetry analysis of the bulk NaCl and the $NaCl_{1/16}$ nano-sample in the temperature range of 293.5−1273.5 K. While the mass loss versus temperature of the $NaCl_{1/16}$ nano-platelets sample decreases monotonically as early as 573 K to reach a relative loss mass of the order of 10% of the original mass around ≈1273 K, the bulk value is about 82.5% in loss mass at the same temperature. By extrapolation, the vaporization temperatures are almost 1686 and 1290 K for bulk NaCl and $NaCl_{1/16}$ nano-platelets sample respectively, i.e. a relative decrease of nearly 23.5%. Figure 7 reports the size dependence of the vaporization temperature $T_V = f(\chi)$ where χ is the relative molar concentration of NaCl of the initial precursor. The net decrease of the vaporization temperature with the size has the following relative concentration dependence:

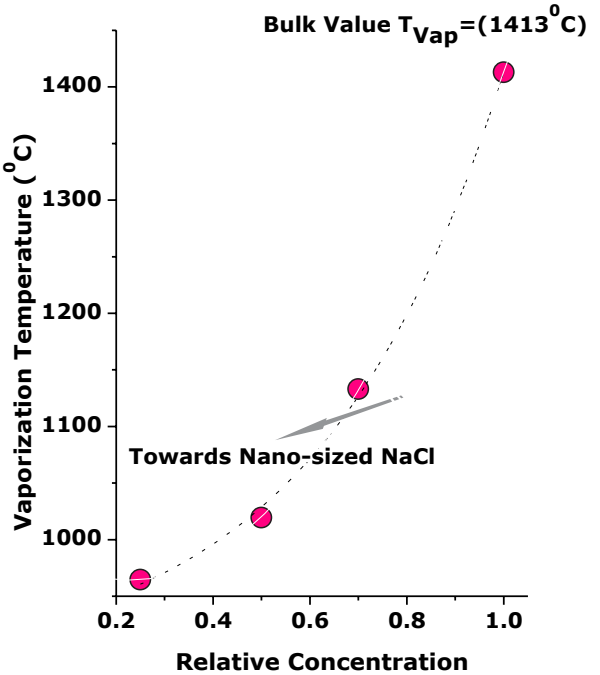

Fig. 7. Size dependence of vaporization temperature of bulk and nano-platelets NaCl.

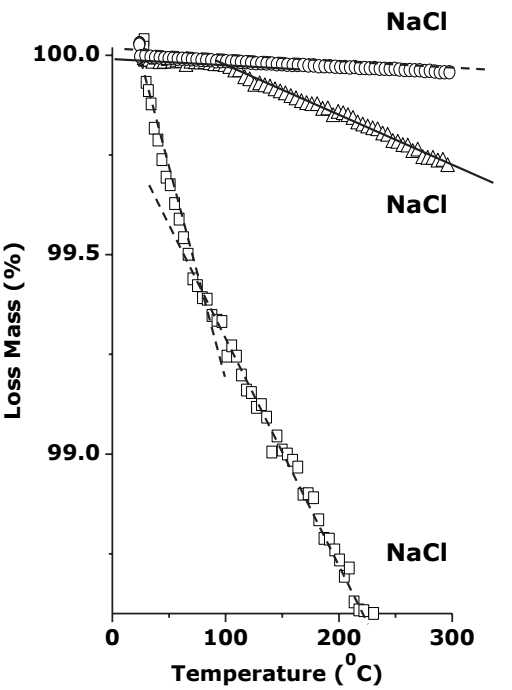

Fig. 8. Zoom thermogravimetry profile of bulk NaCl and nano-platelets NaCl "$NaCl_{1/4}$ and $NaCl_{1/16}$ samples" in the temperature range of 25−250°C.

$T_V(^\circ C) \approx 750.7\chi^2 - 340.1\chi + 1002$. This important size dependence of the vaporization temperature of NaCl is undoubtedly related to surface effects. This trend should be correlated to the results obtained by Samorjai *et al.*[19] It was found that the dislocation density in NaCl crystals strongly affects the vaporization rate. These dislocations could be regarded as extra-generated surfaces. If such a size effect in NaCl nano-crystals is as sizeable as in the case of numerous metallic and semiconducting nano-materials,[6,7] its behavior is firmly peculiar at low temperatures, more specifically in the range of ≈ 25°C−150°C. As indicated in Fig. 8, the mass loss exhibits an obvious nonlinear trends. Since, this nonlinearity of $T_V(\chi)$ is situated in the region of H_2O vaporization temperature, it could be ascribed to the surface adsorbed H_2O molecules at the NaCl nano-crystals. The explanation of such a succinct phenomenon is not understood. As pointed out previously, this size effect on the vaporization temperature, is associated with surface vibrational modes as well as possibly with the collapse of the 3D structural symmetry. Besides these two major sources, the observed T_V size evolution should certainly be concerned by surface Arrhenius activation energy considerations. Actually, in nano-crystalline form, the NaCl surface activation energy, is remarkably low, 0.3 to 0.6 eV.[20] This low surface activation energy has been found consistent with transitions occurring through a sequence of surface diffusion steps. Such a phenomenon coupled with the current observed T_V^{NaCl} lowering with size could indicate that, likely, surface diffusion is, also, an important mechanism for low temperature structural transitions.

3. Conclusion

While this contribution was targeting the possibility to stabilize the metallic CsCl form of nano-sized sodium chloride crystals, it reports, for the first time in the scientific literature, induced size effects in their vaporization properties. The sharp-edged NaCl platelets which are micron-sized in the basal plane (≈1−1.7 μm), reveal nano-scaled features in the transversal direction (minimum of ≈13.5 nm). The standard rocksalt structure has been observed as the dominant crystallographic phase for all investigated NaCl nano-platelets. No CsCl type or a lower symmetry phase transition has been observed with size so

far. In reverse, the nano-sized NaCl platelets showed an obvious surface expansion of different reticular plans. The average lattice parameter $\langle a \rangle$ is about 5.628 ± 0.003 and 5.641 ± 0.003 Å for bulk and nano-sized NaCl crystals, respectively. This stress effect corresponds to a relative increase in volume of the order of $DV/V \approx 0.7\%$. In terms of induced size effects on vaporization temperature T_V, this later decreases from 1686 (bulk value) to nearly 1290 K for NaCl nano-platelets. Such a relative decrease of 23.5% is attributed to surface effects as corroborated by room temperature infrared spectroscopy measurements. The observed H_2O and OH modes as well as other vibrational surface modes, with the collapse of 3D symmetry, are possible origins in lowering of the vaporization temperature. Similarly, the NaCl nano-platelets showed a nonlinear behavior with temperature in the range of $\approx 93.5-423.5$ K. It is suggested that such a nonlinearity could be ascribed to surface adsorbed H_2O molecules and/or surface diffusion phenomenon.

Acknowledgments

This research program was financially supported by the National Research Foundation of South Africa, iThemba LABS, the African Laser Centre as well as the Abdus Salam ICTP within the framework of the NANOAFNET (NANOsciences African NETwork). The staff of the CSIR National Centre for Nanostructured Materials is warmly acknowledged for their valuable scientific and technical contributions.

References

1. A. W. Hull, *Phys. Rev.* **9** (1917) 84.
2. C. Sella and J. J. Trillat, in *Single Crystal Films*, eds. M. H. Francombe and H. Sato (Pergamon Press, 1964).
3. A. Sugawara and K. Mae, *J. Cryst. Growth.* **237–239** (2002) 201−205.
4. J. G. Roberts, S. Hoffer and G. A. Samorjai, *Surf. Sci.* **437** (1999) 75.
5. W. Ernst, M. Eichman, H. Pfnur, K.-L. Jonas, V. Von Oeynhasusen and K. H. Meiwes-Broer, *Appl. Phys. Lett.* **80** (2002) 2595.
6. H. Akbarzadeh, *J. Sci. Technol.* **20** (1996) 409.
7. K. P. Thakur and B. D. Dwary, *J. Phys. C, Solid State Phys.* **19** (1986) 3069.
8. W. D. Halperin, *Rev. Mod. Phys.* **58** (1986) 533.
9. J. Ph. Buffat, *Phys. Rev. A* **13** (1976) 2287.
10. A. Heidenreich, J. Jortner and I. Oref, *J. Chem. Phys.* **97** (1992) 197.
11. U. Landman, D. Scharf and J. Jortner, *Phys. Rev. Lett.* **54** (1985) 1860.
12. D. Scharf, J. Jortner and U. Landman, *J. Chem. Phys.* **87** (1987) 2716.
13. J. P. Rose and R. S. Berry, *J. Chem. Phys.* **96** (1992) 517.
14. K. K. Sunil and K. D. Jordan, *Chem. Phys. Lett.* **164** (1989) 509.
15. D. Patterson, J. A. Morisson and F. Thompson, *Canadian J. Chem.* **33** (1955) 240.
16. J. E. Campana, T. M. Barlak, R. J. Colton, J. J. Decorpo, J. R. Wyatt and B. I. Dunlap, *Phys. Rev. Lett.* **47** (1981) 1046.
17. T. P. Martin, *Phys. Rep.* **95** (1983) 176.
18. R. L. Whetten, *Acc. Chem. Res.* **26** (1993) 49.
19. J. E. Lesker and G. A. Samorjai, *Appl. Phys. Lett.* **12** (1968) 216.
20. R. Hudgins, Ph. Dugourd, J. M. Tanenbaum and M. F. Jarold, *Phys. Rev. Lett.* **78** (1997) 4213.
21. L. F. Audrieth, *Gmelins Handbuch der anorganischen Chemie: Natrium*, Vol. 21, 8th edn. (Verlag-Chemie, Berlin, 1928).
22. O. Miesbauer, M. Gotzinger and W. Peukert, *Nanotechnology* **14** (2003) 371.
23. A. Folch, P. Gorostiza, J. Servat, J. Tejada and F. Sanz, *Surf. Sci.* **380** (1997) 427.